Excessively tilted fiber grating based vector magnetometer

TEAN LU,[1] YUEZHEN SUN,[1] YARIEN MORENO,[1,4] QIZHEN SUN,[1] KAIMING ZHOU,[2,3] HUSHAN WANG,[3] ZHIJUN YAN,[1,2,3,*] DEMING LIU,[1] AND LIN ZHANG,[2]

[1]*School of Optical and Electronic Information, National Engineering Laboratory for Next Generation Internet Access System, Huazhong University of Science and Technology, Wuhan 430074, China*
[2]*Aston Institute of Photonic Technologies (AIPT), Aston University, Birmingham B4 7ET, UK*
[3]*State Key Laboratory of Transient Optics and Photonics, Xi'an Institute of Optics and Precision Mechanics, Chinese Academy of Sciences, Xi'an 710119, China*
[4]*Faculty of Engineering, University of Panama, Panama City, Republic of Panama*
**Corresponding author: yanzhijun@gmail.com*

Received XX Month XXXX; revised XX Month, XXXX; accepted XX Month XXXX; posted XX Month XXXX (Doc. ID XXXXX); published XX Month XXXX

A compact optic-fiber vector magnetometer is proposed and experimentally demonstrated, which is based on an excessively tilted fiber grating (Ex-TFG) assistant with magnetic fluid (MF). Without any complicated processing, the cladding mode resonances of the bare Ex-TFG packaged by MF show high sensitivity to slight perturbations by the magnetic field. Due to the excellent magneto-optical properties of MF and the azimuth-dependent RI sensitivity of Ex-TFG, such magnetometer can achieve both the intensity and orientation detection of magnetic field, which the intensity sensitivity of 2.45nm/mT and the orientation sensitivity of 0.41nm/deg, respectively. And based on the spectral interrogation, the detection limit of the magnetic field intensity could reach around 8.1μT at the minimum wavelength measurement accuracy of 0.02nm.

http://dx.doi.org/10.1364/OL.99.099999

A magnetometer or magnetic sensor is an important instrument to measure magnetism, which plays a crucial role in the applications of biomedical engineering, vehicle monitoring, geological prospecting, submarine hunting and so on [1]. Compared with the traditional magnetometers based on electronic systems, the optic-based technology has outstanding advantages in magnetic sensing, including compact size, high sensitivity, tolerance to harsh environments and ease of integration. However, because of the electromagnetic immunization nature of optical fiber, the traditional optical fiber-based sensors can only detect the temperature, strain and surrounding refractive index, which can't directly measure the magnetic field. To achieve magnetic field measurement, various technologies have been applied, such as utilizing Faraday rotation in a terbium-doped fiber [2], coating magnetostrictive thin films on fiber gratings [3], integrating magnetic fluids (MFs) with various fiber devices and so on. In general, the optical fiber-based sensors would need to be modified by functional materials, such as nickel [4], TbFeCo [5], MF, etc. Among them, MFs have excellent magnetic-optical properties including tunable refractive index (RI), thermal lens-effect and birefringence [6, 7]. Utilizing the RI tunability of MF under magnetic field, researchers have reported many types of optical fiber-based magnetometer, such as fiber Mach-Zehnder interferometers [8], Fabry–Perot interferometers [9], U-bent fibers [10], photonic crystal fibers (PCFs) [11] and long period fiber gratings (LPFGs) [12]. However, all these magnetometers are scalar sensors, which only detect magnetic intensity, and cannot detect direction of magnetic field. Magnetic field is a vector field, which contains not only intensity information but also direction information. Hence, it is important to detect both the intensity and orientation of magnetic field. Based on the anisotropic property of MFs under the magnetic field, so far, several MFs-based optical fiber sensors have been proposed to achieve the vector magnetic measurement. For example, through eccentric fusion splicing, Yin et al. presented a vector magnetometer in three-dimensional space [13, 14]. Jiang et al. reported a high sensitivity vector magnetic field sensor by using side-polished fiber [15]. However, polish and eccentric fusion splicing greatly weaken the mechanical strength of fiber, and raise uncertainties that could not meet repeatability in practical production and application. Lin et al. proposed a two-dimensional vector magnetic field sensor based on tilted fiber Bragg grating (TFBG), which has low sensitivity and measurement accuracy based on intensity interrogation [16]. Then Zhang et al. proposed a vector magnetometer based on surface plasmon resonance and a gold-coated TFBG [17]. Though SPR can benefit the improvement of sensitivity, nanometer-scale metal coating would complicate the process of fabrication and increase costs. Therefore, there is an urgent need to design a magnetic field sensor possessing the

advantages of vector monitoring, simple structure, high sensitivity and reproducibility.

The Ex-TFGs were first reported by Zhou et al. in 2006 [18], which have the related long period and large tilt angle compared with TFBG. Because of asymmetric structure and relative longer period, the Ex-TFGs show polarization-dependent mode coupling behavior, and couple the forward propagating TM and TE core modes into forward propagating TM and TE cladding modes, respectively [19]. The polarization related coupling property promoted the grating to be applied as twisting [20] and transverse loading sensors [21]. Besides of these, Ex-TFGs have high RI sensitivity and low temperature sensitivity [22], and in the experiment, we find the Ex-TFGs have orientation-dependent RI sensitivity, which can be employed to achieve vector field detection, such as the magnetic and electrical field. In this letter, we propose a vector magnetometer based on the Ex-TFG integrated with magnetic fluid, which could achieve both the intensity and orientation measurement of the external magnetic field. The experiment results show that such vector magnetometer has the magnetic field intensity sensitivity of 2.45nm/mT and the orientation sensitivity of 0.41nm/deg. And based on the minimum wavelength measurement accuracy of the interrogation system (0.02nm), the detection limit of the magnetic field intensity is around 8.1μT.

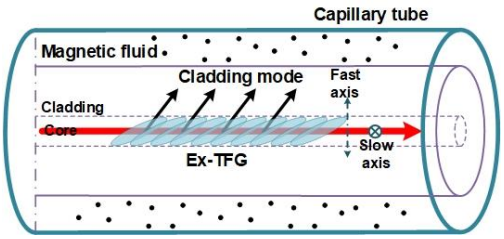

Fig. 1. The schematic diagram of the proposed sensor.

The configuration of Ex-TFG based vector magnetometer is shown in Fig. 1, in which the Ex-TFG was encapsulated in the capillary tube filled with MF (EMG 705). Both ends of the capillary were sealed by glue to prevent leakage. In this work, the Ex-TFGs were UV inscribed in H_2-loaded fiber by using a frequency-doubled Ar^+ laser and the amplitude-mask scanning technique. And the amplitude mask with a period of 5μm was tilted at 80° with respect to the normal of fiber axis, to generate a 28.8μm axial grating period, which would ensure that the cladding modes resonantly excited in the C-L band [13]. The transmission spectrum of the grating at two orthogonal polarizations is plotted in Fig. 2(a), in which could observe four pairs of dual-peaks at the wavelength range between 1450nm and 1650nm. Before integrating with MFs, the RI sensing performance of the Ex-TFG is evaluated with different RI from 1.33 to 1.39 along the fast and slow axis of grating, respectively. The fast and slow axis of grating have been marked in Fig.1. And the results are plotted in Figs. 2(b) and 2(c), in which experiment results show that the Ex-TFGs have orientation-dependent RI sensitivity. The RI sensitivity of TM peak at 1.38 (the RI of MFs is around 1.38) along the slow axis of grating is around 846nm/RIU, which is twice of the one along the fast axis of grating (402nm/RIU). Such azimuth-dependent RI sensitivity promotes that the Ex-TFGs could be employed to detect the dielectrically anisotropic of MFs under the magnetic field.

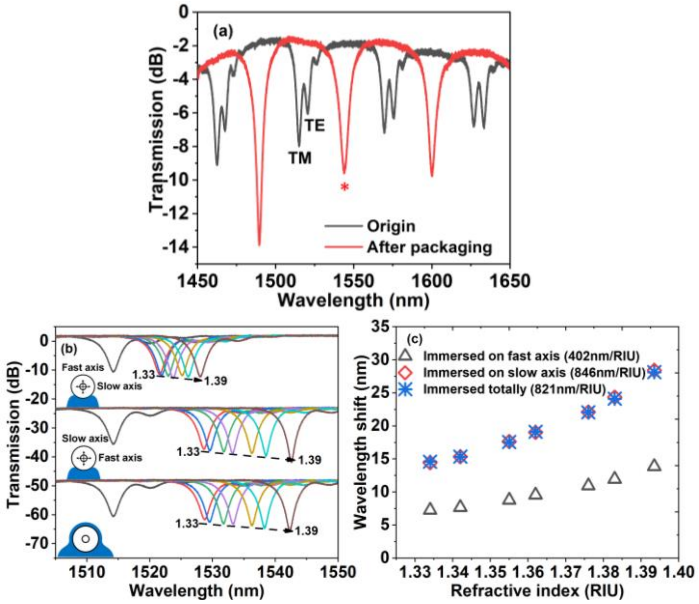

Fig. 2. (a) The transmission spectra of the Ex-TFG originally (black) and after packaging (red, the peak marked by a red asterisk "*" was chosen for vector magnetic sensing); (b) the spectral responses to RI along the fast and slow axis of Ex-TFG; (c) the wavelength shift versus different RI.

According to our previous work, the cladding modes excited by the Ex-TFG are closely related to the RI of the MF around the grating region, and the TM cladding mode has a higher RI sensitivity than the one of the TE cladding mode. At the high RI, the TM and TE peak would overlap together. Therefore, the dual-peak of Ex-TFG disappear after immersed into the MF, and only one resonance peak appears in the transmission spectrum, as seen in Fig. 2(a).

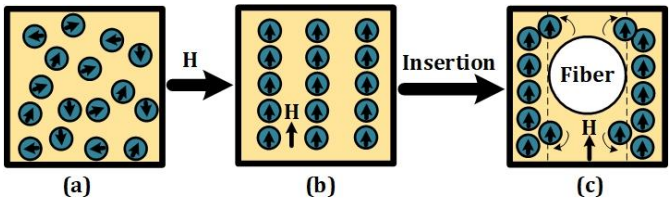

Fig. 3. The schematic diagram of MF (a) without magnetic field, (b) under magnetic field, (c) while inserting a fiber.

MF is a kind of stable suspension made of magnetic particles highly dispersed in a liquid carrier [23]. Without applied magnetic field (H=0), the ferromagnetic particles are randomly distributed, and the fluid is dielectrically isotropic [Fig. 3(a)]. When $H \neq 0$, ferromagnetic particle moments become oriented along the magnetic field and form magnetic chain clusters, resulting in that the fluid becomes dielectrically anisotropic. And along the magnetic field direction, the MF has high particle concentration, which owns high RI [24]; at the normal of magnetic field direction, the MF has lower RI [Fig. 3(b)]. The direction of magnetic field could be determined by detecting the direction of high RI. Due to the

diamagnetic property of the optical fiber, when fiber is inserted into the MF, the ferromagnetic nanoparticles tend to deviate from the upper and underneath surfaces and cluster on the left and right surfaces of the fiber under the magnetic field [Fig. 3(c)], thus, the refractive index around the fiber in the direction of the magnetic field is higher than that in the direction perpendicular to the magnetic field [13,14,17]. Based on the anisotropic distribution of nanoparticles around the fiber and the azimuth-dependent RI sensitivity of the Ex-TFG, we can achieve an optical fiber vector magnetometer and measure the intensity and orientation of magnetic field simultaneously.

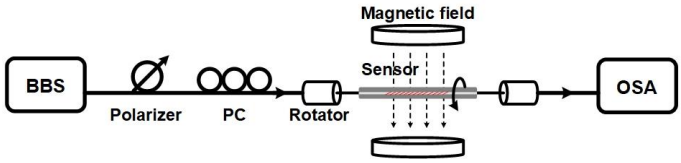

Fig. 4. The experimental setup of the magnetic sensing system.

The experimental setup of the magnetic sensing system is shown in Fig. 4. The interrogation system is based on spectral analysis, which consists of broadband light source (BBS), polarizer, two fiber rotators, polarization controller (PC) and optical spectrum analyzer (OSA). The PC is used to control the polarization state of light launched into Ex-TFG. The uniform magnetic field generated by parallel plate magnets is subjected perpendicularly to the fiber sensor section. The intensity of magnetic field is adjusted by changing the distance between two parallel plate magnets and calibrated by a Gauss meter with a resolution of 0.1mT. The rotators are used to fix and adjust the direction of fiber sensor section from 0° to 360° with respect to the magnetic field, here, the initial position (0°) is defined as the slow axis of Ex-TFG parallel to the magnetic field.

To verify vector magnetic sensing property, we have investigated the orientationally sensing performance of Ex-TFGs based vector magnetometer by rotating the grating from 0° to 360° with a 15° increment under a constant uniform magnetic field. During the sensing process, the light polarization launched into the Ex-TFG is controlled to eliminate the effect of twist on polarization after each rotation by adjusting the PC. Fig. 5(a)-(d) have shown the transmission spectrum of Ex-TFG based vector magnetometer with the different azimuth of optical fiber sensing section under 6mT magnetic field intensity, which can be observed that the evolution of the spectrum exhibits regular and repeatable results. As shown in Figs. 5(a) and (c), the resonance peak of Ex-TFG is red-shift to the longer wavelength as rotating the fiber sensing section from 0° to 90°, and from 180° to 270°. Conversely, the resonance peak shifts to the shorter wavelength as the sensing section rotated from 90° to 180°, and from 270° to 360°, as shown in Figs 5(b) and (d). The above phenomena are in good consistent with the previous analysis, which can be explained that the nanoparticles mostly agglomerate on the sides of fiber that parallel to the magnetic field, causing a higher RI than other regions, and the maximum RI sensitivity of Ex-TFG corresponds to the direction of slow axis so that it is predominate in sensing performance. Thus, when the slow axis of Ex-TFG parallel with magnetic field, the resonance wavelength shifts to minimum, and for the perpendicular situation, it shifts to the minimal resonance wavelength. With the same procedures, the directional sensitivities at different magnetic intensity, 6mT and 12mT, are also characterized, the results of which are depicted in the polar coordinate system [Fig. 5(e)]. As shown clearly in the figure, we could see that the responses of wavelength shift for rotate angle both exhibit an "8" shape, obviously, the higher magnetic field intensity, the stronger orientation dependence, indicating that more nanoparticles lead to more RI change. Furthermore, they both show that the wavelength shifts around 90° (270°) are larger than that around 0° (180°), providing the maximal orientation sensitivities with 0.27nm/deg and 0.41nm/deg under 6mT and 12mT, respectively.

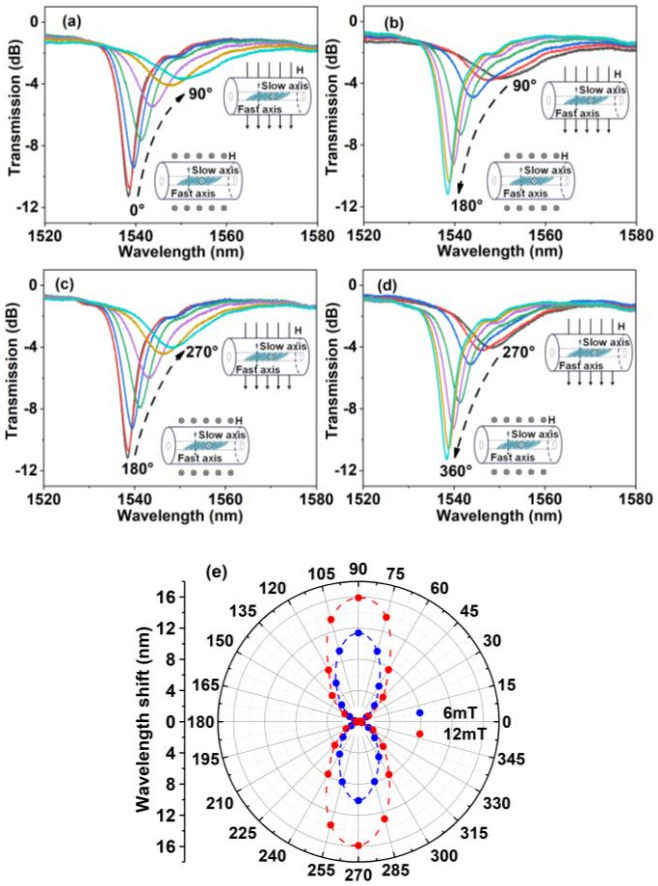

Fig. 5. The transmission spectral responses (a), (b), (c), (d) to the different orientation from 0° to 360° under a magnetic field intensity of 6mT; (e) wavelength shift as a function of magnetic field orientation in polar coordinate system under fixed magnetic field intensities as 6mT and 12mT, respectively.

After verifying orientationally sensing, we have conducted an experiment to investigate the magnetic field intensity response, which can be measured with the increasing magnetic field intensity while fixing three different intersection angles θ between the slow axis of Ex-TFG and the orientation of magnetic field (0°, 45°, 90°). The spectral and wavelength shift responses are shown in Figs. 6(a)-(d), which indicate that when the magnetic field is parallel with slow axis, there is a blue-shift with a sensitivity of -0.33nm/mT (0mT-20mT), on the contrary, resonance wavelength shows a red-shift in vertical condition with a maximum sensitivity of 2.45nm/mT (0mT-13mT), and when the slow axis is oriented at 45°

relative to the magnetic field, the sensor shows a low sensitivity of 0.07nm/mT (0mT-20mT). These differences of sensitivity and detection range result from the movement of nanoparticles with the increasing magnetic field intensity and the sensitivity characteristic of Ex-TFG. According to our analysis, when the slow axis of the Ex-TFG parallels with magnetic field (0°), nanoparticles around the slow axis gradually decrease with increasing magnetic field intensity, leading to the decrease in RI. On the contrary, the nanoparticles gradually accumulate around slow axis for the perpendicular situation (90°), resulting in an increase in RI. And as for 45° position, the number of nanoparticles has no obvious change with the increasing magnetic field intensity, thus, presenting the insensitive response. Moreover, it has the highest sensitivity in vertical condition (90°), but the smallest detection range compared to other conditions, which results from that resonance peak would disappear, as the RI of MF is larger than the mode effective index when magnetic field intensity is over 13mT. The sensitivities obtained in this work are higher than that of most sensor configurations based on MF and varied fiber structures, such as a PCF infiltrated with MF (0.11nm/mT) [25], Mach-Zehnder interferometer (0.222nm/mT) [13], TFBG based on SPR (1.8nm/mT) [17].

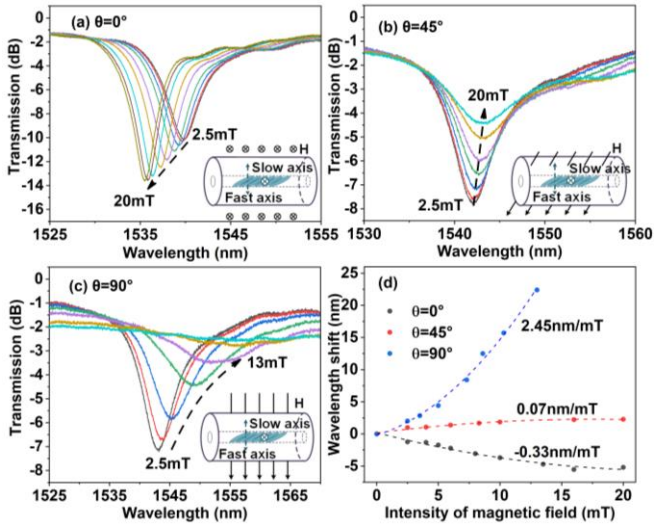

Fig. 6. The transmission spectral responses (a), (b), (c) to the different magnetic field intensity at three different relative direction between slow axis of Ex-TFG and magnetic field (0°, 45°, 90°); (d) wavelength shift versus magnetic field intensity with intersection angle θ of 0°, 45° and 90°.

In conclusion, a vector magnetometer based on an Ex-TFG packaged within MF has been experimentally demonstrated. By utilizing azimuth-dependent RI sensitivity of Ex-TFG and anisotropic distribution of MF, the sensor shows superior performance with the capability of magnetic field orientation and intensity sensing. The experimental results confirm that the sensitivities to magnetic field orientation and intensity can reach as high as 0.41nm/deg and 2.45nm/mT, respectively, and the detection limit of the magnetic field intensity can reach 8.1μT. Moreover, the proposed sensor owns the advantages of high sensitivity, vector monitoring, simple structure, good reproducibility, which has great potential in many fields such as aerospace, military, industry, power transmission system and so on.

Funding.

This work was supported by National Natural Science Foundation of China (No. 61505244, 61605239) and the Fundamental Research Funds for the Central Universities, HUST: 2017KFYXJJ033; the Science Fund for Creative Research Groups of the Nature Science Foundation of Hubei (NO. 2018CFA004), the Major Projects of Technical Innovation of Hubei (NO. 2018AAA040).

References

1. K. Khanafer, K. Vafai, Heat Mass Transf. **42,** 939 (2006).
2. L. Sun, S. Jiang, and J. R. Marciante, Opt. Express. **18,** 5407 (2010).
3. M. Yang, J. Dai, C. Zhou, and D. Jiang, Opt. Express. **17,** 20777 (2009).
4. G. Vértesy, A. Gasparics, and Z. Vértesy, J. Magn. Magn. Mater. **196-197,** 333 (1999).
5. M. Yang, J. Dai, X. Li, and J. Wang, J. Appl. Phys. **108,** 033102 (2010).
6. S. Yang, J. Chieh, H. Horng, C.-Y. Hong, and H. Yang, Appl. Phys. Lett. **84,** 5204 (2004).
7. Z. Di, X. Chen, S. Pu, X. Hu, and Y. Xia, Appl. Phys. Lett. **89,** 211106 (2006).
8. Z. Li, C. Liao, J. Song, Y. Wang, F. Zhu, Y. Wang, and X. Dong, Photonics Res. **4,** 197 (2016).
9. Y. Zhao, R.-Q Lv, Y. Ying, and Q. Wang, Opt. Laser Technol. **44,** 899 (2012).
10. T. Liu, Y. Chen, Q. Han, and X. Lv, IEEE Photonics J. **6,** 5300307 (2014).
11. Y. Chen, Q. Han, W. Yan, Y. Yao, and T. Liu, IEEE Photonics Technol. Lett. **28,** 2665 (2016).
12. Y. Miao, H. Zhang, J. Lin, B. Song, K. Zhang, W. Lin, B. Liu, and J. Yao, Appl. Phys. Lett. 106, 132410 (2015).
13. J. Yin, P. Yan, H. Chen, L. Yu, J. Jiang, M. Zhang, and S. Ruan, Appl. Phys. Lett. **110,** 231104 (2017).
14. J. Yin, S. Ruan, T. Liu, J. Jiang, S. Wang, H. Wei, and P. Yan, Sens. Actuators B Chem. **238,** 518 (2017).
15. Z. Jiang, J. Dong, S. Hu, Y. Zhang, Y. Chen, Y. Luo, W. Zhu, W. Qiu, H. Lu, H. Guan, Y. Zhong, J. Yu, J. Zhang, and Z. Chen, Opt. Lett. **43,** 4743 (2018).
16. W. Lin, Y. Miao, H. Zhang, B. Liu, Y. Liu, B. Song, and J. Wu, J. Lightwave Technol. **31,** 2599 (2013).
17. Z. Zhang, T. Guo, X. Zhang, J. Xu, W. Xie, M. Nie, Q. Wu, B. O. Guan, and J. Albert, Appl. Phys. Lett. **108,** 101105 (2016).
18. K. Zhou, L. Zhang, X. Chen, and I. Bennion, Opt. Lett. **31,** 1193 (2006).
19. Z. Yan, H. Wang, C. Wang, Z. Sun, G. Yin, K. Zhou, Y. Wang, W. Zhao, and L. Zhang, Opt. Express. **24,** 12107 (2016).
20. X. Chen, K. Zhou, L. Zhang, and I. Bennion, IEEE Photonics Technol. Lett. **18,** 2596 (2006).
21. R. Suo, X. Chen, K. Zhou, L. Zhang, and I. Bennion, Meas. Sci. Technol. **20,** 034015 (2009).
22. Z. Yan, Q. Sun, C. Wang, Z. Sun, C. Mou, K. Zhou, D. Liu, and L. Zhang, Opt. Express. **25,** 3336 (2017).
23. G. Bertoni, B. Torre, A. Falqui, D. Fragouli, A. Athanassiou, and R. Cingolani, J. Phys. Chem. C. **115,** 7249 (2011).
24. S. V. Kredentser, M. M. Kulyk, V. M. Kalita, K. Y. Slyusarenko, V. Yu. Reshetnyak, and Yu. A. Reznikov, Soft Matter. **13,** 4080 (2017).
25. A. Mahmood, V. Kavungal, S. S. Ahmed, G. Farrell, and Y. Semenova, Opt. Lett. **40**, 4983 (2015).

1. K. Khanafer, K. Vafai, "The role of porous media in biomedical engineering as related to magnetic resonance imaging and drug delivery," Heat Mass Transf. **42,** 939 (2006).
2. L. Sun, S. Jiang, and J. R. Marciante, "All-fiber optical magnetic-field sensor based on Faraday rotation in highly terbium-doped fiber," Opt. Express. **18**(6), 5407-5412 (2010).
3. M. Yang, J. Dai, C. Zhou, and D. Jiang, "Optical fiber magnetic field sensors with TbDyFe magnetostrictive thin films as sensing materials," Opt. Express. **17**(23), 20777-20782 (2009).
4. G. Vértesy, A. Gasparics, and Z. Vértesy, "Improving the sensitivity of Fluxset magnetometer by processing of the sensor core," J. Magn. Magn. Mater. **196-197,** 333-334 (1999).
5. M. Yang, J. Dai, X. Li, and J. Wang, "Side-polished fiber Bragg grating refractive index sensor with TbFeCo magnetoptic thin film," J. Appl. Phys. **108,** 033102 (2010).
6. S. Yang, J. Chieh, H. Horng, C.-Y. Hong, and H. Yang, "Origin and applications of magnetically tunable refractive index of magnetic fluid films," Appl. Phys. Lett. **84,** 5204 (2004).
7. Z. Di, X. Chen, S. Pu, X. Hu, and Y. Xia, "Magnetic-field-induced birefringence and particle agglomeration in magnetic fluids," Appl. Phys. Lett. **89,** 211106 (2006).
8. Z. Li, C. Liao, J. Song, Y. Wang, F. Zhu, Y. Wang, and X. Dong, "Ultrasensitive magnetic field sensor based on an in-fiber Mach–Zehnder interferometer with a magnetic fluid component," Photonics Res. **4,** 197-201 (2016).
9. Y. Zhao, R.-Q Lv, Y. Ying, and Q. Wang, "Hollow-core photonic crystal fiber Fabry–Perot sensor for magnetic field measurement based on magnetic fluid," Opt. Laser Technol. **44,** 899-902 (2012).
10. T. Liu, Y. Chen, Q. Han, and X. Lv, "Magnetic Field Sensor Based on U-Bent Single-Mode Fiber and Magnetic Fluid," IEEE Photonics J. **6,** 5300307 (2014).
11. Y. Chen, Q. Han, W. Yan, Y. Yao, and T. Liu, "Magnetic-Fluid-Coated Photonic Crystal Fiber and FBG for Magnetic Field and Temperature Sensing," IEEE Photonics Technol. Lett. **28,** 2665-2668 (2016).
12. Y. Miao, H. Zhang, J. Lin, B. Song, K. Zhang, W. Lin, B. Liu, and J. Yao, "Simultaneous measurement of temperature and magnetic field based on a long period grating concatenated with multimode fiber," Appl. Phys. Lett. 106, 132410 (2015).
13. J. Yin, P. Yan, H. Chen, L. Yu, J. Jiang, M. Zhang, and S. Ruan, "All-fiber-optic vector magnetometer based on anisotropic magnetism-manipulation of ferromagnetism nanoparticles," Appl. Phys. Lett. **110,** 231104 (2017).
14. J. Yin, S. Ruan, T. Liu, J. Jiang, S. Wang, H. Wei, and P. Yan, "All-fiber-optic vector magnetometer based on nano-magnetic fluids filled double-clad photonic crystal fiber," Sens. Actuators B Chem. **238,** 518-524 (2017).
15. Z. Jiang, J. Dong, S. Hu, Y. Zhang, Y. Chen, Y. Luo, W. Zhu, W. Qiu, H. Lu, H. Guan, Y. Zhong, J. Yu, J. Zhang, and Z. Chen, "High-sensitivity vector magnetic field sensor based on side-polished fiber plasmon and ferrofluid," Opt. Lett. **43,** 4743-4746 (2018).
16. W. Lin, Y. Miao, H. Zhang, B. Liu, Y. Liu, B. Song, and J. Wu, "Two-Dimensional Magnetic Field Vector Sensor Based on Tilted Fiber Bragg Grating and Magnetic Fluid," J. Lightwave Technol. **31,** 2599-2605 (2013).
17. Z. Zhang, T. Guo, X. Zhang, J. Xu, W. Xie, M. Nie, Q. Wu, B. O. Guan, and J. Albert, "Plasmonic fiber-optic vector magnetometer," Appl. Phys. Lett. **108,** 101105 (2016).
18. K. Zhou, L. Zhang, X. Chen, and I. Bennion, "Optic sensors of high refractive-index responsivity and low thermal cross sensitivity that use fiber Bragg gratings of >80° tilted structures," Opt. Lett. **31,** 1193-1195 (2006).
19. Z. Yan, H. Wang, C. Wang, Z. Sun, G. Yin, K. Zhou, Y. Wang, W. Zhao, and L. Zhang, "Theoretical and experimental analysis of excessively tilted fiber gratings," Opt. Express. **24**(11), 12107-12115 (2016).
20. X. Chen, K. Zhou, L. Zhang, and I. Bennion, "In-Fiber Twist Sensor Based on a Fiber Bragg Grating With 81◦ Tilted Structure," IEEE Photonics Technol. Lett. **18,** 2596-2598 (2006).
21. R. Suo, X. Chen, K. Zhou, L. Zhang, and I. Bennion, "In-fibre directional transverse loading sensor based on excessively tilted fibre Bragg gratings," Meas. Sci. Technol. **20**(3), 034015 (2009).
22. Z. Yan, Q. Sun, C. Wang, Z. Sun, C. Mou, K. Zhou, D. Liu, and L. Zhang, "Refractive index and temperature sensitivity characterization of excessively tilted fiber grating," Opt. Express. **25**(4), 3336-3346 (2017).
23. G. Bertoni, B. Torre, A. Falqui, D. Fragouli, A. Athanassiou, and R. Cingolani, "Nanochains formation of superparamagnetic nanoparticles," J. Phys. Chem. C. **115**(15), 7249-7254 (2011).
24. S. V. Kredentser, M. M. Kulyk, V. M. Kalita, K. Y. Slyusarenko, V. Yu. Reshetnyak, and Yu. A. Reznikov, "Magneto-induced anisotropy in magnetic colloids of superparamagnetic magnetite nanoparticles in an external magnetic field," Soft Matter. **13**(22), 4080-4087 (2017).
25. A. Mahmood, V. Kavungal, S. S. Ahmed, G. Farrell, and Y. Semenova, "Magnetic-field sensor based on whispering-gallery modes in a photonic crystal fiber infiltrated with magnetic fluid," Opt. Lett. **40**, 4983-4986 (2015).